

Accepted Manuscript

Benchmarking of laboratory evolved unspecific peroxygenases for the synthesis of human drug metabolites

Patricia Gomez de Santos, Fadia V. Cervantes, Florian Tieves, Francisco J. Plou, Frank Hollmann, Miguel Alcalde



PII: S0040-4020(19)30151-6

DOI: <https://doi.org/10.1016/j.tet.2019.02.013>

Reference: TET 30136

To appear in: *Tetrahedron*

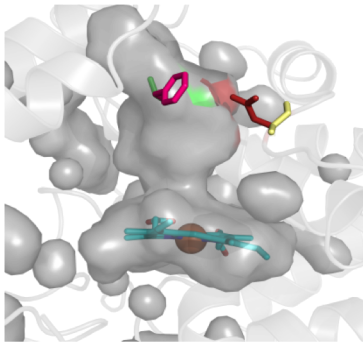
Received Date: 2 November 2018

Revised Date: 28 January 2019

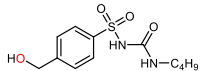
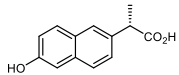
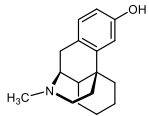
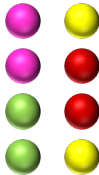
Accepted Date: 5 February 2019

Please cite this article as: Gomez de Santos P, Cervantes FV, Tieves F, Plou FJ, Hollmann F, Alcalde M, Benchmarking of laboratory evolved unspecific peroxygenases for the synthesis of human drug metabolites, *Tetrahedron* (2019), doi: <https://doi.org/10.1016/j.tet.2019.02.013>.

This is a PDF file of an unedited manuscript that has been accepted for publication. As a service to our customers we are providing this early version of the manuscript. The manuscript will undergo copyediting, typesetting, and review of the resulting proof before it is published in its final form. Please note that during the production process errors may be discovered which could affect the content, and all legal disclaimers that apply to the journal pertain.



Position
191 241



Ref n°: TET-D-18-01678
Revised version
Tetrahedron
28/01/19

Benchmarking of laboratory evolved unspecific peroxygenases for the synthesis of human drug metabolites

Patricia Gomez de Santos^{1†}, Fadia V. Cervantes^{1†}, Florian Tieves[§], Francisco J. Plou^{†‡},
Frank Hollmann[§] and Miguel Alcalde^{†‡*}

¹ These authors contributed equally to this work.

[†]Department of Biocatalysis, Institute of Catalysis, CSIC, 28049 Madrid, Spain.

[‡]EvoEnzyme, S.L., C/Marie Curie n°2, 28049 Madrid, Spain.

[§]Department of Biotechnology, Delft University of Technology, van der Massweg 9,
2629HZ Delft, The Netherlands.

* Correspondence should be addressed to: M. A. (malcalde@icp.csic.es).

ABSTRACT

By mimicking the role of human liver P450 monooxygenases, fungal unspecific peroxygenases (UPOs) can perform a range of highly selective oxyfunctionalization reactions on pharmacological compounds, including O-dealkylations and hydroxylations, thereby simulating drug metabolism. Here we have benchmarked human drug metabolite (HDM) synthesis by several evolved UPO mutants, focusing on dextromethorphan, naproxen and tolbutamide. The HDM from dextromethorphan was prepared at the semi-preparative scale as a proof of production. The structural analysis of mutations involved in the synthesis of HDMs highlights the heme access channel as the main feature on which to focus when designing evolved UPOs. These variants are becoming emergent tools for the cost-effective synthesis of HDMs from next-generation drugs.

KEYWORDS: unspecific peroxygenase, human drug metabolites, dextromethorphan, tolbutamide, naproxen, heme access channel.

1. Introduction

Synthetic chemistry is increasingly being incorporated into pipelines to discover new bioactive compounds, with new drugs being designed on the basis of better understanding the appropriate biological targets.¹ The US Food and Drug Administration (FDA) guidelines for metabolites in safety testing (MIST) declare that any metabolite that is generated above 10% of the parent drug should be subject to safety testing.² Therefore, it is fundamental for the pharma industry to produce large amounts of pure metabolites (human drug metabolites, HDMs) in order to be able to perform pharmacokinetic and pharmacodynamics studies. However, low yields and the cumbersome processes associated with their chemical synthesis are important drawbacks to the production of HDMs, with enzymes representing the most feasible option to overcome such barriers.

Unspecific peroxygenases (UPOs; EC 1.11.2.1) are extracellular heme-thiolate enzymes considered by many as the “generational successors” to P450s for selective C-H oxyfunctionalization and they are of particular interest in organic synthesis. Using H₂O₂ as the final electron acceptor and exclusive oxygen donor, UPOs perform dozens of two-electron oxidation (mono(per)oxygenations) reactions.³ Indeed, these enzymes have proven to be a valuable departure point for the synthesis of HDMs.^{4,5,6} We previously performed directed evolution on the UPO from the basidiomycete *Agrocybe aegerita* (*AaeUPO*) to enhance its functional heterologous expression and activity in yeast.^{7,8} The secretion variant of this evolution campaign (named PaDa-I), harbored five mutations in the mature protein that improved its biochemical attributes (V57A-L67F-V75I-I248V-F311L), and four further mutations in the signal peptide that increased secretion. In a later study, the PaDa-I mutant was evolved for the selective synthesis of 1-naphthol, generating the JaWa variant that carried two additional mutations (G241D-R257K).⁹ More recently, JaWa was further evolved to SoLo mutant (containing the F191S substitution) in order to synthesize the HDM 5'-

hydroxypropranolol from the beta-blocker propranolol on a semi-preparative scale (Figure 1).^{10,11}

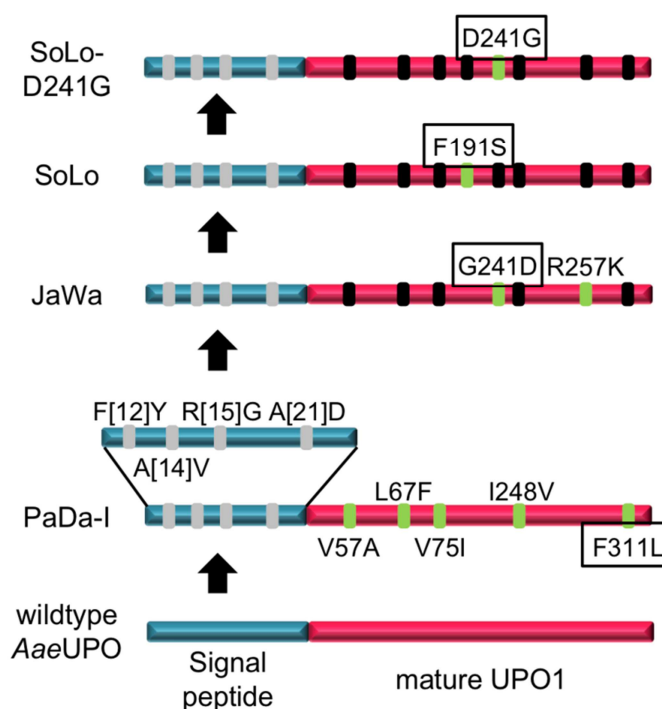


Figure 1: Evolved variants used in the current study. The signal peptide is represented in blue and the mature protein in pink, along with the different mutations: green rectangles identify new mutations; black rectangles highlight the accumulated mutations; and grey rectangles indicate the mutations in the signal peptide. PaDa-I, JaWa and SoLo mutants come from previous work⁷⁻¹¹ whereas SoLo-D241G has been designed in the current study.

In addition, we have also explored how to enhance stability and how to expand the substrate promiscuity of this versatile biocatalyst by structure-guided evolution¹² and neutral genetic drift.¹³ Consequently, we believe that the extensive portfolio of UPO variants we have generated in recent years is likely to open new avenues for the more efficient synthesis of HDMs.

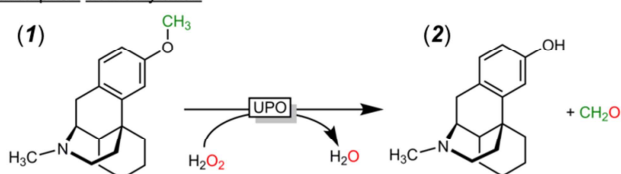
In the current study, we have tested several evolved UPO variants for their capacity to synthesize authentic HDMs from three consolidated pharmaceutical agents: dextromethorphan, naproxen and tolbutamide. For each synthetic reaction, the evolved UPOs were systematically benchmarked and dextrophan synthesis was taken to a semi-preparative scale. The differences in substrate preferences of the evolved UPOs

were analyzed within a mutational context through site-directed mutagenesis and they were further discussed.

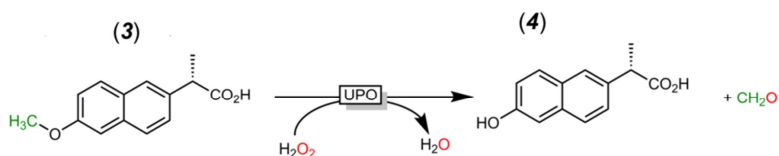
2. Results and discussion

The evolved PaDa-I, JaWa and SoLo UPO mutants were produced and purified to homogeneity (Reinheitszahl –Rz- $A_{418}/A_{280} \sim 2.2$), and their activity was tested on dextromethorphan (**1**), an antitussive drug with sedative and dissociative properties. Native *Aae*UPO converts this pharmaceutical agent into dextrorphan (**2**) by O-dealkylation, its authentic HDM (**Figure 2**).⁵

A. Dextromethorphan demethylation



B. Naproxen demethylation



C. Tolbutamide hydroxylation

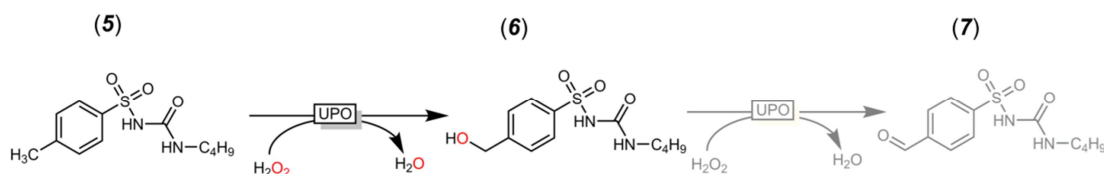


Figure 2: Drugs transformed by UPOs and their corresponding products. (A) *Aae*UPO transforms dextromethorphan (**1**) to dextrorphan (**2**) or (B) naproxen (**3**) to O-desmethylnaproxen (**4**) by O-dealkylation. (C) Stepwise conversion of tolbutamide (**5**) into 4-hydroxymethyl-tolbutamide (**6**) is achieved by attacking the benzylic carbon, although it may be subsequently overoxidised to 4-formyl-tolbutamide (**7**).

Previous engineered P450 BM3 variants were tested towards (**1**) but the product obtained was not the authentic HDM (**2**)^{14,15}. The reactions of the selected UPO mutants were analyzed by HPLC/PDA (**Figure 3**) and the products determined by

HPLC/MS (see **Experimental Section**). In all cases, the substrate conversion indicated that each of the mutants outperformed the native *AaeUPO* (16%): PaDa-I, 57%; SoLo 75%; and JaWa, 82% (**Table 1**).

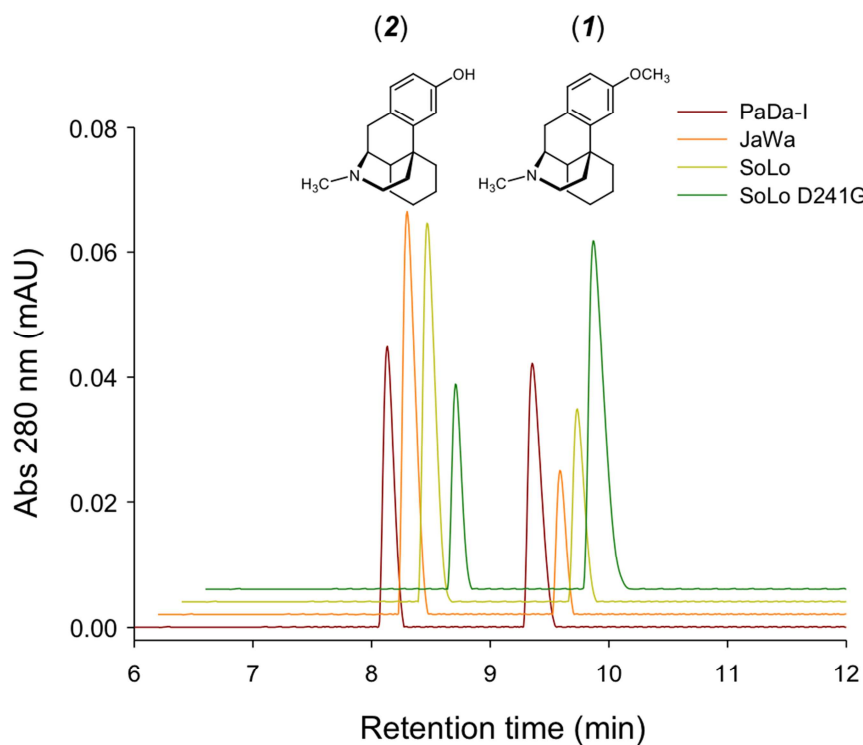


Figure 3: Dextromethorphan conversion by evolved UPOs. HPLC elution profiles after a 60 min reaction time: (1) dextromethorphan; (2) dextrorphan.

Table 1. Substrates converted to described products confirmed by mass spectrometry.

Substrate (m/z)	Product (m/z)	PaDa-I (% product)	JaWa (% product)	SoLo (% product)	<i>AaeUPO</i> * (% product)	SoLo-D241G (% product)
Dextromethorphan [M+H] ⁺ 272	Dextrorphan [M+H] ⁺ 258	57	82	75	16	37
Naproxen [M-H] ⁻ 229	O-desmethylnaproxen [M-H] ⁻ 215	36	25	12	57	25
Tolbutamide [M+H] ⁺ 271	4-hydroxymethyl-tolbutamide [M+H] ⁺ 287	20	14	19	15	21
	4-formyl-tolbutamide [M+H] ⁺ 285	15	-	4	n.q.	16

Reactions were performed at room temperature for one hour (after enzyme activity decreased). Each reaction mixture contained 0.1 μ M of purified enzyme, 1 mM substrate (dissolved in 10% acetonitrile), 4 mM ascorbic acid, and 1mM H₂O₂ in 100 mM potassium phosphate buffer pH 7.0 (1 mL final volume). *data obtained from⁵. (-): not detected n.q.: not quantified. TTNs for mutants can be calculated from the ratio between product conversion and enzyme concentration after 1 h reaction (*i.e.* multiplying each value of product conversion by 100). Standard errors were in all cases lower than 3%.

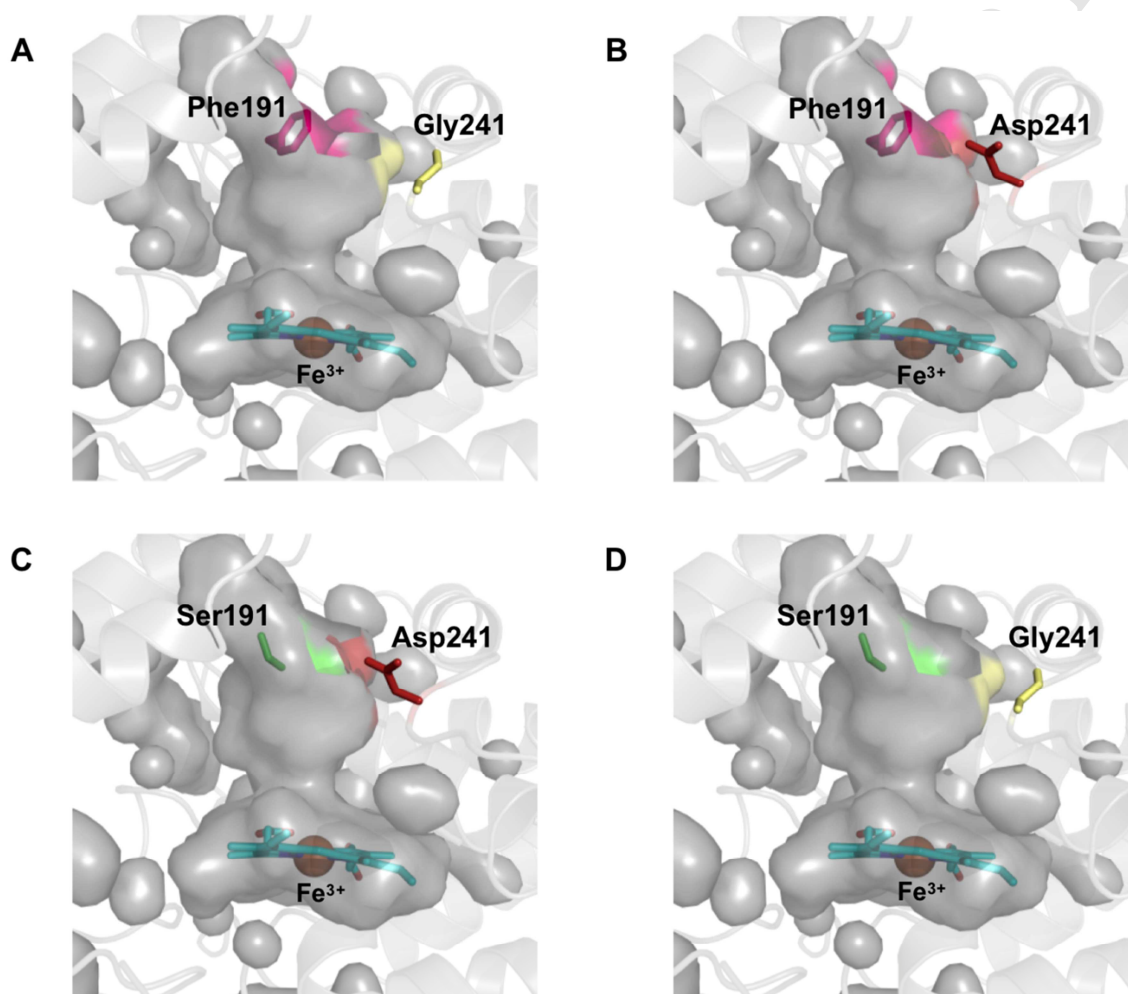
Given its excellent behavior under operational conditions during the synthesis of the HDM 5'-hydroxypropranolol¹⁰, the SoLo variant was then evaluated further on a semi-preparative scale. By applying a gradual supply of H₂O₂ to avoid oxidative

damage, we produced up to 102.1 mg of (**2**) from (**1**), with a yield of 75.2% (see **Experimental Section** for details). We then tested the selective demethylation of naproxen (**3**), a non-steroidal anti-inflammatory drug, achieving the highest substrate conversion with the PaDa-I secretion variant (36%), followed by JaWa (25%) and SoLo (12%), yet in all the cases less than that of the native *AaeUPO* (57%) (**Table 1**) but higher than previous reported P450 variants.¹⁶

We also assayed tolbutamide (**5**), a Na⁺-channel blocker, the hydroxylation of which was mediated by *AaeUPO* through the attack of the benzylic carbon, giving rise to the HDM 4-hydroxymethyl-tolbutamide (**6**) (**Figure 2**). In this case the substrate conversion were 20%, 14%, 19% and 15% for PaDa-I, JaWa, SoLo and native *AaeUPO*, respectively (**Table 1**). Although JaWa was associated with the lowest conversion, it did display a notable lack of overoxidation (*i.e.*: a further two-electron oxidation reaction of (**6**) to 4-formyl-tolbutamide (**7**)), which may be an important property when considering the large-scale production and purification of (**6**). The total turnover numbers (TTNs, reported as $\mu\text{mol product}/\mu\text{mol enzyme}$) for each evolved mutant and reaction were within the same range, from 1200 (for SoLo in the production of *O*-desmethylnaproxen) to 8200 (for JaWa in the production of dextrorphan) (**Table 1**).

The striking differences in substrate conversion between the distinct evolved variants, generated over 8 rounds of directed evolution, led us to analyze the role of the mutations located around the catalytic cavity (**Figures 1, 4**). The heme channel of *AaeUPO* is furnished with 10 aromatic residues, of which Phe76 and Phe191 define its access, while Phe69, Phe121 and Phe199 are involved in positioning the substrate for catalysis.¹⁷ In the crystal structure of the PaDa-I variant recently made available, we noted that the F311L mutation is implicated in broadening the access channel, and it is also responsible for the dual conformational state of Phe191, conferring unheralded plasticity to the heme entrance in some of the evolved UPO variants.¹⁸ Such flexibility

at the heme access channel is not a feature of the native *AaeUPO* and accordingly, it is reasonable to think that this modifications might explain the improved yields with dextromethorphan (**1**) given its bulk. It is also worth noting that JaWa and SoLo produced higher yields with (**1**) than PaDa-I, differences that could be attributed to the G241D mutation situated at the entrance of the heme channel that is carried by both



JaWa and SoLo but that is absent in PaDa-I.

Figure 4: The heme access channel of the evolved UPOs. PaDa-I (A), JaWa (B), SoLo (C) and SoLo-D241G (D). The UPO structures are shown as a light grey cartoon with the heme access channel/pocket as a grey surface, and the relevant amino acids are indicated in pink (Phe191), yellow (Gly241), dark red (Asp241) and green (Ser191). The model was visualized with Pymol (<http://pymol.org>) based on the crystal structure of the PaDa-I mutant at a resolution of 1.5 Å, PDB entry: 5OXU.

In our previous evolution experiments with JaWa and SoLo, computational analysis revealed that G241D favored substrate anchoring (for naphthalene and

propranolol, respectively), better orientating these substrates for oxygenation. To confirm that this beneficial effect also applies to (**1**), we reverted the G241D mutation in SoLo by site-directed mutagenesis. The SoLo-D241G mutant produced much lower conversion from (**1**) (from 75% to 37%), albeit still above those of native AaeUPO (16%, **Table 1**). The SoLo-D241G mutant also showed lower product formation than PaDa-I (37% vs. 57%), indicating that the F191S mutation in SoLo must be responsible for this effect, which is again consistent with the small differences between the JaWa (lacking F191S mutation) and SoLo mutants (**Figure 4**). In terms of naproxen (**3**) conversion, the effect of reverting the G241D mutation was the opposite of that observed for (**1**), increasing roughly two-fold in the case of SoLo-D241G (**Table 1**). As indicated previously, positions 191 and 241 seem to be crucial for this phenomenon, with Phe191 and Gly241 of PaDa-I representing the best combination for this substrate among the evolved variants. Finally, when tolbutamide (**5**) was tested as the substrate, the three mutants rendered similar amounts of hydroxytolbutamide (**6**). Interestingly, PaDa-I showed a 15% overoxidation activity on (**6**), producing 4-formyl-tolbutamide (**7**), while SoLo and JaWa generated only traces of this product. The reverted SoLo-D241G variant also produced similar conversions to SoLo in terms of (**5**) hydroxylation (21 and 19%, respectively), although this variant enhanced overoxidation to the levels seen with PaDa-I (**Table 1**). This difference might indicate that the G241D mutation shortens the residence time of (**6**) in the heme cavity, thereby suppressing overoxidation.

3. Conclusions

Evolved UPO variants with different substrate scopes are suitable biocatalysts to synthesize known and novel HDMs. The heme access channel of these evolved variants is malleable and it can be adapted through additional evolutionary campaigns to achieve cost-effective production of HDMs. Accordingly, future structure-guided evolution experiments focusing on this region may expand the substrate range of UPOs towards next-generation drugs with different chemical structures.

4. Experimental

Tolbutamide, ascorbic acid and Yeast Transformation kit were purchased from Sigma-Aldrich/Merck (Darmstadt, Germany). Naproxen, dextromethorphan, dextrorphan were purchased from Santa Cruz Biotechnology (CA, USA). The high-fidelity DNA polymerase iProof was acquired from BioRad (CA, USA). The BamHI and XhoI restriction enzymes were purchased from New England Biolabs (MA, USA) and the protease-deficient *S. cerevisiae* strain BJ5465 from LGCPromochem (Barcelona, Spain). The Zymoprep Yeast Plasmid Miniprep kit and Zymoclean Gel DNA Recovery kit were from Zymo Research (CA, USA). The NucleoSpin Plasmid kit was purchased from Macherey–Nagel (Düren, Germany) and the oligonucleotides were synthesized by IDT (IA, USA). All chemicals were reagent-grade purity or analytical standards.

4.1. Expression and purification of UPO variants

UPO variants were produced and purified as described before.^{8, 10}

4.2. Reactions and product characterization

Reaction mixtures (1 mL) contained purified peroxygenases (PaDa-I, JaWa, SoLo and SoLo-D241G mutants, 0.1 μ M), substrate (1 mM, dissolved in 10% acetonitrile), potassium phosphate buffer (100 mM, pH 7.0), ascorbic acid (4 mM) and a single dosage of H₂O₂ (1 mM). All reactions were stirred at 30°C for one hour until reaction stopped. The reaction mixtures were analyzed by reversed-phase chromatography (HPLC) using a quaternary pump (Agilent Technologies, model 1100) coupled to a Phenomenex Zorbax Eclipse plus C18 column (4.6 mm diameter by 100 mm length, 3.5 μ m particle size), with an autosampler (Hitachi, model L-2200) and a photodiode array detector (PDA, Varian Prostar). Column temperature was kept at 30°C and flow rate at 1 mL/min. Each injection had a volume of 10 μ L and the analytes were eluted with a gradient from 100% of CH₃CN to 100% of H₂O in 5 minutes (with 0.1% vol/vol of formic acid in both solvents), followed by 10 minutes linear gradient

from 100% of H₂O to 100% of CH₃CN. UV detection wavelengths were 238 nm for tolbutamide, 280 nm for dextromethorphan and 235 nm for naproxen. Integration of peaks was carried out using the Varian Star LC workstation 6.41.

Identification of reaction products was determined by liquid chromatography-mass spectrometry (HPLC/MS) with a Waters Instrument equipped with a chromatographic module Alliance 2695, diode array detector (PDA 2996) and a quadrupole mass spectrometer (Micromass ZQ). Reversed phase chromatography was performed on a SunFire C18 (2.1 mm diameter, 50 mm length, 3.5 μm particle size, Waters); which was eluted at 1 mL/min with aqueous/acetonitrile (0.1% vol/vol formic acid in both solvents), with 20 minutes linear gradient from 95% of acetonitrile to 95% of H₂O. Samples were ionized by electrospray ionization (ESI, with nitrogen to desolvate the mobile phase) and analyzed in positive reflector mode. Naproxen and O-desmethylnaproxen were analyzed employing a mass spectrometer coupled to a hybrid QTOF analyzer (model QSTAR, Pulsari, AB Sciex). The compounds were analyzed by direct infusion and ionized by ESI in negative reflector mode. The ionizing phase was methanol basified with 1% NH₄OH.

4.3. Semi-preparative production of dextromethorphan and NMR analysis

Dextromethorphan (135.6 mg, 0.5 mmol) was dissolved in acetonitrile (10 mL). The solution was added to potassium phosphate buffer (90 mL, 100 mM pH 7.0) containing ascorbic acid (4 mmol) and SoLo mutant (0.05 μmol). Reactions (2 × 50 mL) were performed at 30°C and 600 rpm using a thermo shaker device (Eppendorf). H₂O₂ was added with a syringe pump (0.06 mmol/h) over 16.5 h. Afterwards, the solution was heated to 70 °C for 3 min and the precipitated enzyme removed. The conversion (76.2%) was determined by HPLC (water with 0.1% TFA/ acetonitrile, 5/95 to 95/5) on Waters Xterra RP18 column (4.6 × 150 mm, 5 μm). For purification, solvents were removed under reduced pressure and freeze drying from the cleared solution. The crude product was washed with methanol, filtered and purified by flash chromatography

(water with 0.1% TFA/ acetonitrile, 5/95 to 95/5) on REVELERIS® C18 column (12 g, 40 μ m). Dextrorphan containing fractions were pooled and the solvents removed under reduced pressure and freeze drying obtaining dextrorphan (102.1 mg, 75.2% yield) as white powder. Dextrorphan: ^1H NMR (400 MHz, methanol- d_4) δ 7.08 (d, J = 8.3 Hz, 1H), 6.80 (d, J = 2.5 Hz, 1H), 6.71 (dd, J = 8.3, 2.5 Hz, 1H), 3.65 – 3.59 (m, 1H), 3.22 – 3.08 (m, 3H), 2.92 (s, 3H), 2.73 (td, J = 13.2, 3.6 Hz, 1H), 2.52 – 2.39 (m, 1H), 1.97 (dt, J = 12.4, 3.1 Hz, 1H), 1.87 (td, J = 13.8, 4.6 Hz, 1H), 1.79 – 1.27 (m, 7H), 1.26 – 1.11 (m, 1H). ^{13}C NMR (101 MHz, methanol- d_4) δ 128.97, 114.04, 60.57, 43.09, 39.84, 39.37, 35.44, 35.02, 25.54, 22.66, 21.41.

4.4 Site-directed mutagenesis at position 241

PCR reactions for reversion of Asp241 were carried out with the primers D241G F (5'-gatttcttccg \underline{c} gcacccagcccgagaag \underline{t} gtacaggagtcgaggtagttgtacagg-3') and D241G R (5'-cctgtacaactacctcgactcctgtaccacttctcgggctgggtg \underline{c} gcggaagaaatc-3'); mutated bases are underlined. The PCR reaction mixtures contained: 1) 50 μ L final volume, DMSO (3%), RMLN (0.5 μ M), D241G F (0.5 μ M), dNTPs (1 mM, 0.25 mM each), high-fidelity DNA polymerase iProof (0.02 U/mL), and the template SoLo (10 ng), and 2) 50 μ L final volume, DMSO (3%), RMLN (0.5 μ M), D241G R (0.5 μ M), dNTPs (1 mM, 0.25 mM each), high-fidelity DNA polymerase iProof (0.02 U/mL), and the template SoLo (10 ng). PCR reactions were carried out on a gradient thermocycler using the following parameters: 98°C for 30 s (1 cycle); 98°C for 10 s, 48°C for 30 s, and 72°C for 30 s (28 cycles); and 72°C for 10 min (1 cycle). PCR products were loaded onto a preparative agarose gel and purified with the Zymoclean Gel DNA Recovery kit. The recovered DNA fragments were cloned under the control of the GAL1 promoter of the pJRoc30 expression shuttle vector, with use of BamHI and XhoI to linearize the plasmid and to remove the parent gene. The linearized vector was loaded onto a preparative agarose gel and purified with the Zymoclean Gel DNA Recovery kit. The PCR products (200 ng

each) were mixed with the linearized plasmid (100 ng) and transformed into *S. cerevisiae* for *in vivo* gene reassembly and cloning by IVOE.¹⁹

Acknowledgements

This work was supported by the Spanish Government Projects BIO2016-79106-R-Lignolition, BIO2016-76601-C3-1-R and CTQ2016-70138-R, the CSIC Project PIE-201580E042, and the Comunidad de Madrid Synergy CAM Project Y2018/BIO-4738-EVOCHIMERA-CM. P. Gomez de Santos thanks the Ministry of Science, Innovation and Universities (Spain) for her FPI scholarship (BES-2017-080040).

References

- [1] National Research Council, Industrialization of Biology: A Roadmap to Accelerate the Advanced Manufacturing of Chemicals, The National Academies Press, Washington, DC, 2015.
- [2] F.P. Guengerich, Introduction: Human Metabolites in Safety Testing (MIST) Issue, *Chem. Res. Toxicol.* **22** (2009) 237-238.
- [3] P. Molina-Espeja, P. Gomez de Santos, M. Alcalde, Directed Evolution of Unspecific Peroxygenase, in: M. Alcalde (Ed.) *Directed Enzyme Evolution: Advances and Applications*, Springer International Publishing, Cham, 2017, pp. 127-143.
- [4] M. Kinne, M. Poraj-Kobielska, E. Aranda, R. Ullrich, K.E. Hammel, K. Scheibner, M. Hofrichter, Regioselective preparation of 5-hydroxypropranolol and 4'-hydroxydiclofenac with a fungal peroxygenase, *Bioorg. Med. Chem. Lett.* **19** (2009) 3085-3087.
- [5] M. Poraj-Kobielska, M. Kinne, R. Ullrich, K. Scheibner, G. Kayser, K.E. Hammel, M. Hofrichter, Preparation of human drug metabolites using fungal peroxygenases, *Biochem. Pharmacol.* **82** (2011) 789-796.
- [6] J. Kiebist, W. Holla, J. Heidrich, M. Poraj-Kobielska, M. Sandvoss, R. Simonis, G. Gröbe, J. Atzrodt, M. Hofrichter, K. Scheibner, One-pot synthesis of human metabolites of SAR548304 by fungal peroxygenases, *Bioorg. Med. Chem.* **23** (2015) 4324-4332.

- [7] P. Molina-Espeja, E. Garcia-Ruiz, D. Gonzalez-Perez, R. Ullrich, M. Hofrichter, M. Alcalde, Directed Evolution of Unspecific Peroxygenase from *Agrocybe aegerita*, *Appl. Environ. Microbiol.* **80** (2014) 3496-3507.
- [8] P. Molina-Espeja, S. Ma, D.M. Mate, R. Ludwig, M. Alcalde, Tandem-yeast expression system for engineering and producing unspecific peroxygenase, *Enzyme Microb. Technol.* **73-74** (2015) 29-33.
- [9] P. Molina-Espeja, M. Cañellas, F.J. Plou, M. Hofrichter, F. Lucas, V. Guallar, M. Alcalde, Synthesis of 1-Naphthol by a Natural Peroxygenase Engineered by Directed Evolution, *ChemBioChem*, **17** (2016) 341-349.
- [10] P. Gomez de Santos, M. Cañellas, F. Tieves, S.H.H. Younes, P. Molina-Espeja, M. Hofrichter, F. Hollmann, V. Guallar, M. Alcalde, Selective Synthesis of the Human Drug Metabolite 5'-Hydroxypropranolol by an Evolved Self-Sufficient Peroxygenase, *ACS Catal.* **8** (2018) 4789-4799.
- [11] P. Molina-Espeja, F.J. Plou, M. Alcalde, P. Gomez de Santos. Mutants of unspecific peroxygenase with high monooxygenase activity and uses thereof. Patent no. WO/2017/081355
- [12] D.M. Mate, M.A. Palomino, P. Molina-Espeja, J. Martin-Diaz, M. Alcalde, Modification of the peroxygenative:peroxidative activity ratio in the unspecific peroxygenase from *Agrocybe aegerita* by structure-guided evolution, *Protein Eng., Des. Sel.* **30** (2017) 191-198.
- [13] J. Martin-Diaz, C. Paret, E. García-Ruiz, P. Molina-Espeja, M. Alcalde, Shuffling the Neutral Drift of Unspecific Peroxygenase in *Saccharomyces cerevisiae*, *Appl. Environ. Microbiol.* **84** (2018) e00808-18.
- [14] J.C. Lewis, S.M. Mantovani, Y. Fu, C.D. Snow, R.S. Komor, C. Wong and F.H. Arnold, Combinatorial Alanine Substitution Enables Rapid Optimization of Cytochrome P450BM3 for Selective Hydroxylation of Large Substrates. *ChemBioChem.* **11** (2010) 2502-2505.

- [15] B.M.A. van Vugt-Lussenburg, M.C. Damsten, D.M. Maasdijk, N.P.E. Vermeulen, J.N.M. Commandeur, Heterotropic and homotropic cooperativity by a drug-metabolising mutant of cytochrome P450 BM3. *Biochem. Biophys. Res. Commun.* **346** (2006) 810-818.
- [16] A. Rentmeister, T.R. Brown, C.D. Snow, M.N. Carbone, F.H. Arnold, Engineered bacterial mimics of human drug metabolizing enzyme CYP2C9. *ChemCatChem*, **3** (2011) 1065-1071.
- [17] K. Piontek, E. Strittmatter, R. Ullrich, G. Gröbe, M.J. Pecyna, M. Kluge, K. Scheibner, M. Hofrichter, D.A. Plattner, Structural Basis of Substrate Conversion in a New Aromatic Peroxygenase: Cytochrome P450 functionality with benefits, *J. Biol. Chem.* **288** (2013) 34767-34776.
- [18] M. Ramirez-Escudero, P. Molina-Espeja, P. Gomez de Santos, M. Hofrichter, J. Sanz-Aparicio, M. Alcalde, Structural insights into the substrate promiscuity of a laboratory-evolved peroxygenase, *ACS Chem. Biol.* **13** (2018) 3259-3268.
- [19] M. Alcalde, Mutagenesis Protocols in *Saccharomyces cerevisiae* by In Vivo Overlap Extension, in: J. Braman (Ed.) *In Vitro Mutagenesis Protocols: Third Edition*, Humana Press, Totowa, NJ, 2010, pp. 3-14.

FIGURE LEGENDS:

Figure 1: Evolved variants used in the current study. The signal peptide is represented in blue and the mature protein in pink, along with the different mutations: green rectangles identify new mutations; black rectangles highlight the accumulated mutations; and grey rectangles indicate the mutations in the signal peptide.

Figure 2: Drugs transformed by UPOs and their corresponding products. (A) AaeUPO transforms dextromethorphan (**1**) to dextrorphan (**2**) or (B) naproxen (**3**) to *O*-desmethylnaproxen (**4**) by *O*-dealkylation. (C) Stepwise conversion of tolbutamide (**5**) into hydroxytolbutamide (**6**) is achieved by attacking the benzylic carbon, although it may be subsequently overoxidised to 4-formyl-tolbutamide (**7**).

Figure 3: Dextromethorphan conversion by evolved UPOs. HPLC elution profiles after a 60 min reaction time: (**1**) dextromethorphan; (**2**) dextrorphan.

Figure 4: The heme access channel of the evolved UPOs. PaDa-I (A), JaWa (B), SoLo (C) and SoLo-D241G (D). The UPO structures are shown as a light grey cartoon with the heme access channel/pocket as a grey surface, and the relevant amino acids are indicated in pink (Phe191), yellow (Gly241), dark red (Asp241) and green (Ser191). The model was visualized with Pymol (<http://pymol.org>) based on the crystal structure of the PaDa-I mutant at a resolution of 1.5 Å, PDB entry: 5OXU.